

Excited State Structure Correlates with Efficient Photoconversion in Unidirectional Motors

Palas Roy,¹ Andy S. Sardjan,² Arjen Cossens,² Wesley R. Browne,² Ben L. Feringa,^{2} and Stephen R. Meech^{1*}*

¹ School of Chemistry, University of East Anglia, Norwich Research Park, Norwich NR4 7TJ, U.K. ² Stratingh Institute for Chemistry, University of Groningen, Nijenborgh 4, 9747AG Groningen, The Netherlands.

Supporting Information

1. Experimental Methods

2. FSRS Signal processing

3. Supporting Figures

Figure S1. Steady state absorption spectra

Figure S2. Transient absorption spectra at different time delays

Figure S3. Peak shift dynamics of dark state transient absorption spectra

Figure S4. The DFT calculated Raman active modes referred to in main text

Figure S5. FSRS spectra at different time delays

Figure S6. Processing procedure for raw FSRS data

Figure S7. Pyramidalization mode coupled to HOOP motion

Figure S8 Time dependent FSRS Peak frequencies

Table S1. Relaxation times recovered from spectral shift dynamics in the dark state

1. Experimental Methods

Materials. The synthesis of compounds 9-(2-methyl-2,3-dihydro-1H-cyclopenta[a]naphthalen-1-ylidene)-9H-fluorene, with substituents (-R): -H, -CN, -Cl, and (-OMe) were reported earlier.¹⁻² Solvents were spectroscopic grade and used as received.

Femtosecond transient absorption measurements (TA). TA is a two pulse technique – a femtosecond pulse is the pump and a time delayed broadband white light continuum is the probe. The detailed description of the transient absorption set up used here has been mentioned elsewhere.³ In brief, the fundamental beam from the Spectra Physics Mai Tai laser oscillator is amplified in a Ti:sapphire regenerative amplifier (Spectra Physics Spitfire ACE) to generate output pulses with duration of 120 fs at 800 nm at a repetition rate of 1 kHz and energy of 5 mJ per pulse. This amplified pulse output drives two commercial optical parametric amplifiers (OPA, Light Conversion TOPAS Prime). One OPA is used to generate the 400 nm pump pulse with duration of 80fs, which electronically excites the samples. The pump pulse was passed through a mechanical chopper (500Hz), a computer controlled delay stage and a half wave plate and polarizer (to set polarization at magic angle). The second OPA is tuned to generate pulses at 1250 nm which was attenuated (10 μ J) and then focused onto a 3 mm thick sapphire window to generate broadband white light continuum (500-1400 nm). The WLC before the sample was split by a 50/50 beam splitter. One part (Reference) was used in the reference detection channel to correct for intensity fluctuations in the probe spectrum. The second part (Probe) was spatially overlapped with the pump pulse in a 1 mm thick sample cell. Both the actinic pump and probe pulses were focused, with focal spot sizes was at 270 μ m and 50 μ m. The sample was circulated through the sample cell which had 0.5 mm thick fused silica windows. Pump beam energy was attenuated to 0.25 mW at the sample cell in order to avoid any photodamage. After passing

through the sample the probe was aligned collinearly with the reference beam on top of each other and both were dispersed using a home built prism based spectrograph. Both the dispersed beams were then focused and detected by two separate synchronised 16 bit A/D CCD detectors from Entwicklungsbüro Stresing (1024 pixels). Chopper at 500Hz in the pump beam path allowed the detection of pump-on/pump-off probe and reference spectra. The referenced difference spectrum for each pulse pair was calculated using:

$$\Delta A = -\log\left(\frac{\text{Probe (Pump on)} \times \text{Reference (Pump off)}}{\text{Reference (Pump on)} \times \text{Probe (Pump off)}}\right)$$

The detector was calibrated using Mercury-Argon lamp (HG-1 Ocean Optics). The instrument response function, IRF with 400 nm excitation pump and was determined to be about 100 fs as obtained from the solvent Kerr response. The data presented was average over 5 cycles and each time trace was accumulated for 1 s. All pump-probe measurements were done under flowing condition with the liquid driven by a peristaltic pump.

Femtosecond Stimulated Raman measurements (FSRS). The same setup used for TA measurement was modified for FSRS measurements.³ FSRS is a three pulse technique: the femtosecond ‘actinic’ pump excites the molecule of interest, which is probed by a narrowband (10 cm⁻¹) picosecond Raman pulse in the presence of a broadband femtosecond probe pulse, which together stimulate the coherent Raman scattering process from the sample. The actinic pump and white-light continuum probe pulses were generated as described in the previous section. The Raman pulse was generated by sending part of the fundamental amplified beam (from Spectra Physics Spitfire ACE amplifier) through a commercial second harmonic bandwidth compressor (SHBC, Light Conversion) and picosecond configured OPA (Light Conversion, TOPAS-PS). The Raman pulse was tuned to be in resonance with the excited state absorption (550-625 nm) for the

dark state of each molecular motor. The spectral resolution for FSRS was limited by the pulse-width of the Raman pump which was set at about 2 ps. All the three beams- Actinic pump, Raman pump and white-light probe pulse are focused (spot sizes 150, 250 and 50 μm respectively) and overlapped spatially and temporally inside the flow cell (no reference Probe was used). Stimulated Raman from cyclohexane was used to optimize temporal overlap between Probe and Raman pump. While actinic pump – Raman probe delay is controlled by a delay stage. The transmitted probe beam was dispersed in a high spectral resolution ($<10\text{ cm}^{-1}$) grating spectrometer (SPEX 500M) and the probe was detected using a single CCD (1024 pixel). The detector was calibrated using Hg-Ar lamp (Ocean Optics). Each spectrum was accumulated for 10 s and a total of 10 scans were recorded using LabView controlled software. The actinic pump power used was 1 mW at 400nm for all four samples. Raman pump was set at 560nm (4 mW) for –OMe and –H; 575 nm (4 mW) for –Cl and 610nm (4mW) for –CN derivatives. All the measurements were done in similar experimental conditions. The sample absorbance (at 400nm) was kept below OD 1 during all measurements. Large volumes (150ml) of sample were used and circulated continuously through a 1mm flow cuvette with the liquid driven by a peristaltic pump to replenish molecule for each pump pulse. The sample integrity of the solution is checked by recording ground state absorption before and after FSRS measurement. Time resolution of the experiment is dictated by the actinic pump and probe pulse timing which is around 100 fs, as obtained from solvent response in methanol.

Spectra were recorded at 1 kHz. Two synchronized choppers operating at 250 Hz and 500 Hz were used to modulate the Raman pump and actinic pulses respectively. This result into four different signals: i) Excited state FSRS (Probe + Raman + Actinic); ii) Transient absorption (Probe +

Actinic); iii) Ground state FSRS (Probe + Raman) and iv) Probe reference (probe only). The FSRS signal processing to obtain excited state Raman is described in the next section.

Steady-state Raman. Steady-state off-resonance Raman spectra were recorded at 532 nm (25 mW, Cobolt lasers) using a laser equipped Olympus BX51 upright microscope dichroic filter at 45 degrees.⁴ Raman scattering was collected and guided by a MM fibre optic to a Shamrock300i spectrograph and Newton EMCCD-BU (Andor Technology). Data was baseline corrected using Spectragryph.⁵

DFT Calculation. Theoretical calculations for Raman spectra of molecular motors have been carried out within Density Functional Theory (DFT) at the rb3lyp/tzvp level using Gaussian16 program.⁶ Each derivative was first optimized for structure and then Raman spectra were calculated. All frequencies have been scaled by a factor of 0.98 (to account for a systematic error in the DFT predictions)⁷ and then plotted as shown by black vertical lines in main Figure 2. Some of the important modes are also shown in SI Figure S4, S7.

Spectral Curve Fitting. The Gaussian peak fittings (for Figure 5) were performed using OriginPro software keeping all the peak widths fixed and varying the peak frequencies. This provides good quality fits for all datasets, with only one Gaussian frequency being time dependent – an example for –H is shown (Figure S8).

The H and Cl derivatives show a well resolved peak frequency red-shift in the 1335-1365 cm^{-1} region. For –OMe and –CN derivatives, the broad mode around 1400 cm^{-1} dominates the line-width, making resolution of the other contributions more challenging. However, the fixed width fittings yields reproducible data which mirrored the behavior seen in the –H and –Cl data sets. Fits with all free parameters (width, peak frequency and amplitude) produced the same behavior

e.g. peak frequency shift (around 1330-1340 cm^{-1} region) for the –CN derivative and no shift (around 1370 cm^{-1} region) for the –OMe derivative – but with greater uncertainty.

2. FSRS Signal Processing

The unprocessed FSRS signal is obtained when Actinic pump, Raman pump and probe pulses are overlapped on the sample as we detect $\log(I_{\text{Raman+Actinic+Probe}}/I_{\text{Probe}})$. Along with excited state Raman, this unprocessed FSRS signal also contains information on ground state Raman ($\log(I_{\text{Raman+Probe}}/I_{\text{Probe}})$), transient absorption (TA) ($\log(I_{\text{Actinic+Probe}}/I_{\text{Probe}})$) and nonlinear background. Therefore the unprocessed FSRS data has subtracted from it ground state Raman and TA contributions as shown in SI Figure S6a. In our experiment, the ground state Raman signal is dominated by solvent contributions, as the Raman pump is nonresonant with the motor derivatives. The resultant difference spectrum is then baseline corrected to obtain the excited state Raman signal, as shown in SI Figure S6b. This same procedure is followed for different pump-probe time delays and FSRS spectra finally obtained for all the motors as shown in the main Figure 3 and SI Figure S5.

3. Supporting Figures

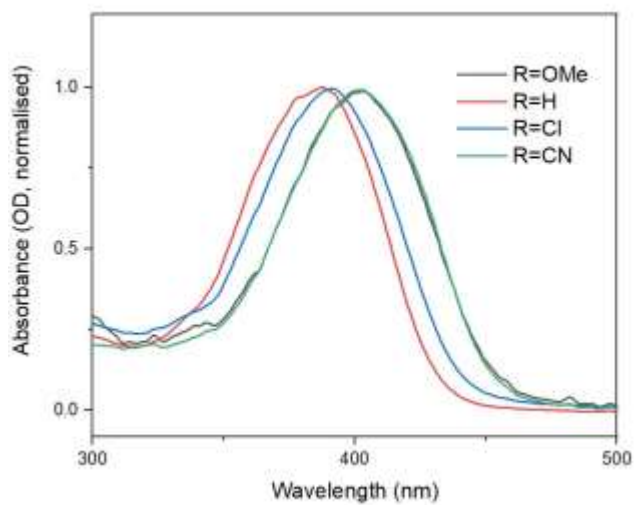


Figure S1. Steady state absorption spectra are shown for the four molecular motor derivatives in methanol.

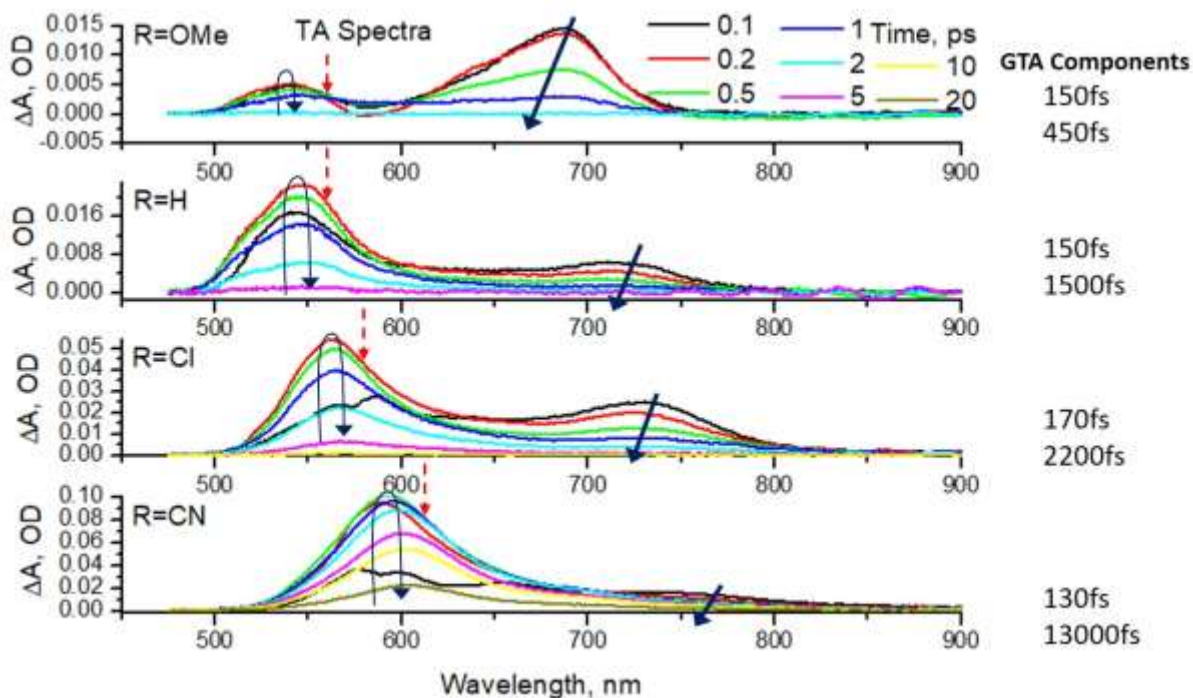


Figure S2. Transient absorption spectra for the four motor derivatives in methanol at different pump-probe delays. The solid arrows represent spectral evolution from bright state to dark state, as discussed previously for $R = H$.³ The most red-shifted transient decays in ca 100 fs as the dark state rises, with the latter subsequently decaying to ground state. The red dash arrows represent Raman pump used for FSRS measurements, which is selected to have a near constant shift from the peak of the dark state TA. The Global target analysis provide the lifetime components.

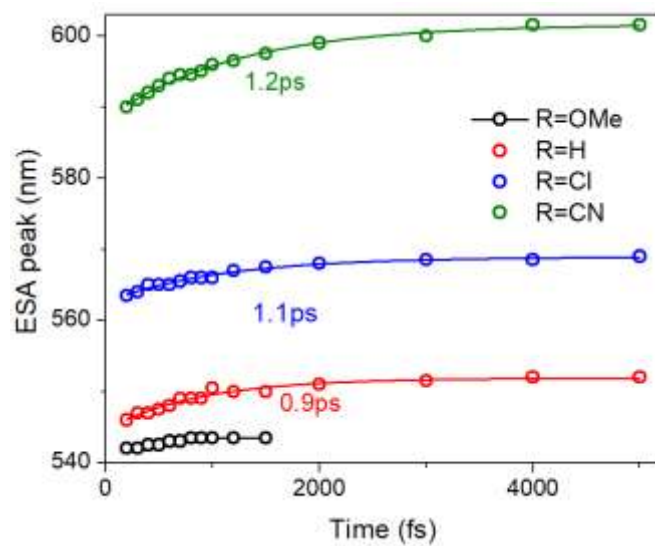


Figure S3. Peak shift of dark state absorption with time for the four derivatives. -CN, -Cl and -H derivatives show peak shift with time constant of ~ 1 ps while -OMe doesn't undergo any significant peak shift.

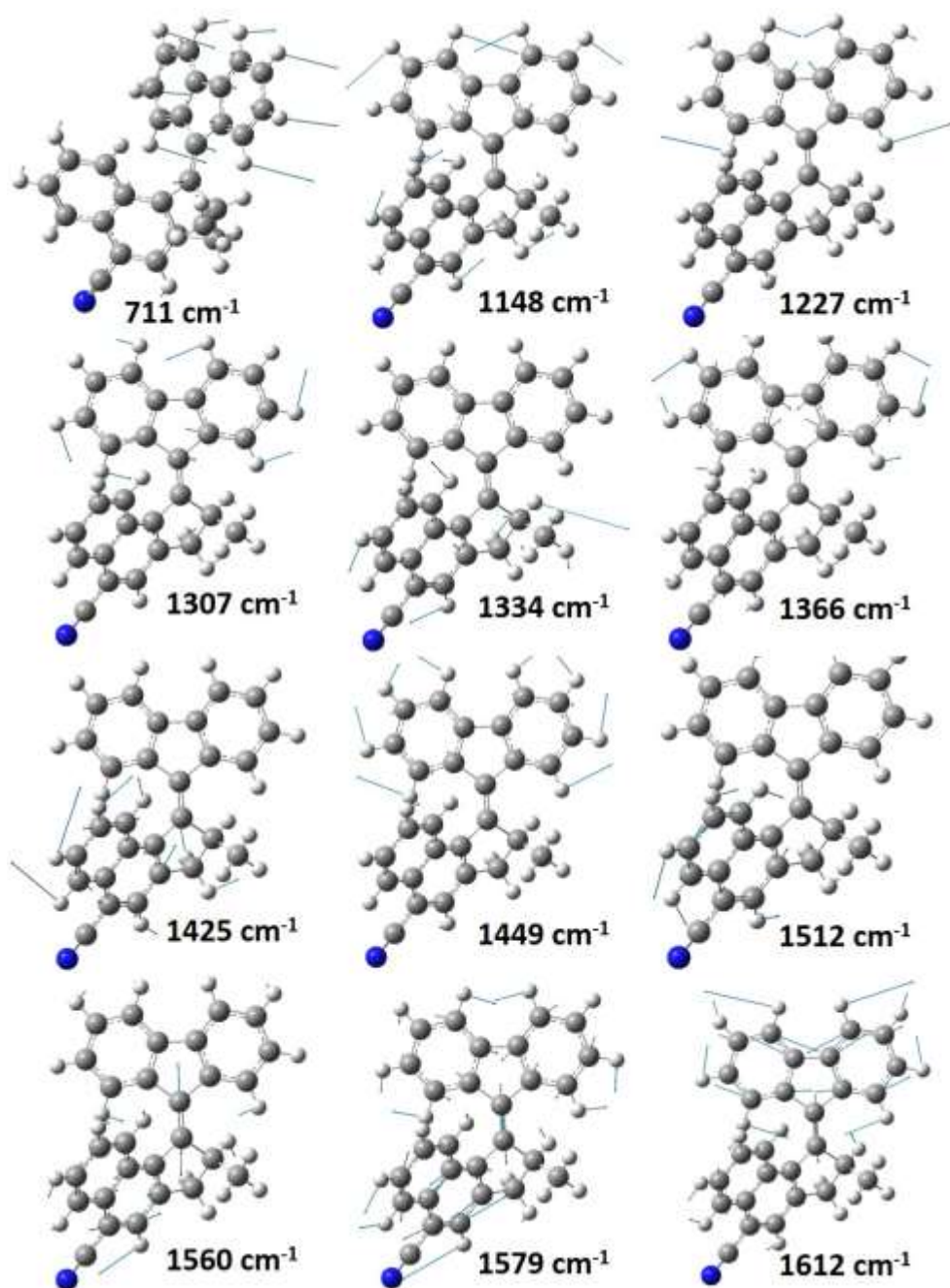


Figure S4. DFT Calculated non-resonant Raman modes for the $-\text{CN}$ derivative. The displacements for the 711, 1148, 1227, 1307, 1334, 1366, 1425, 1449, 1512, 1560, 1579, and 1612 cm^{-1} modes are shown, which are representative of those for all derivatives discussed in the text.

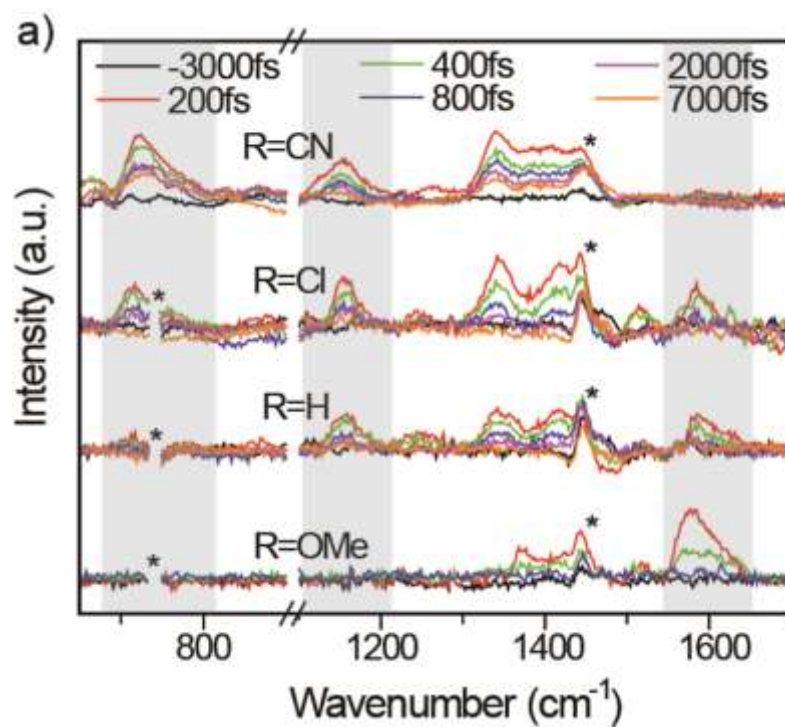


Figure S5. FSRS data of the four motor derivatives at different time-delays. Regions marked * solvent and instrumental artifacts. Shaded areas represent area of interest.

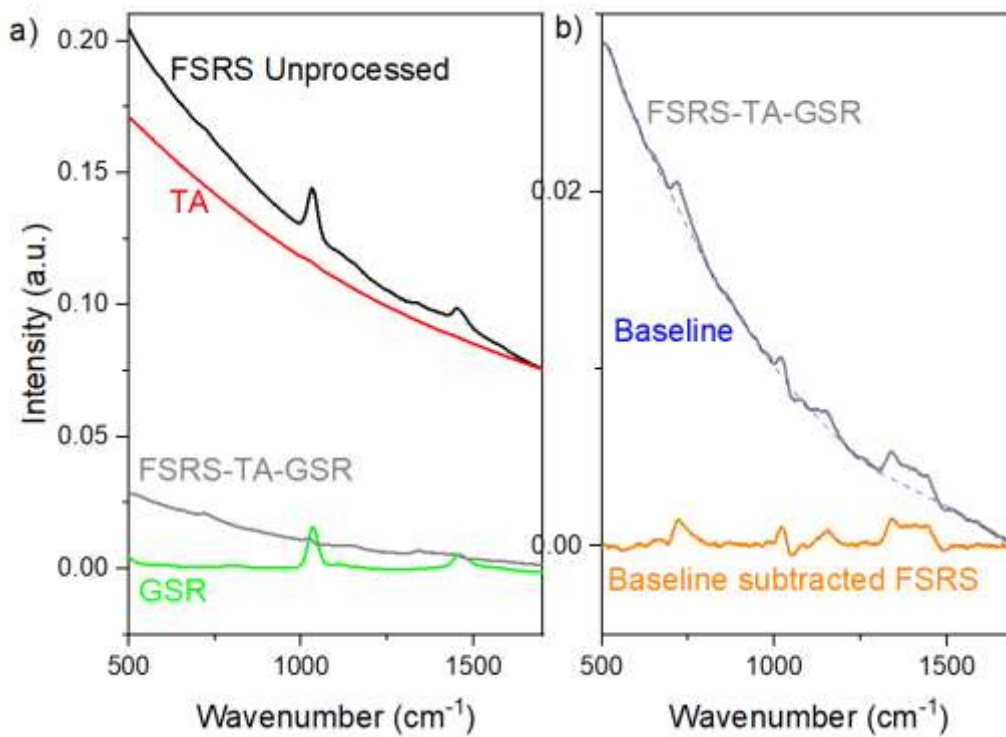


Figure S6. Processing raw FSRS signal a) by removing contribution from transient absorption (TA) and ground state Raman (GSR) and then b) the difference spectra is corrected for baseline which yields the excited state Raman.

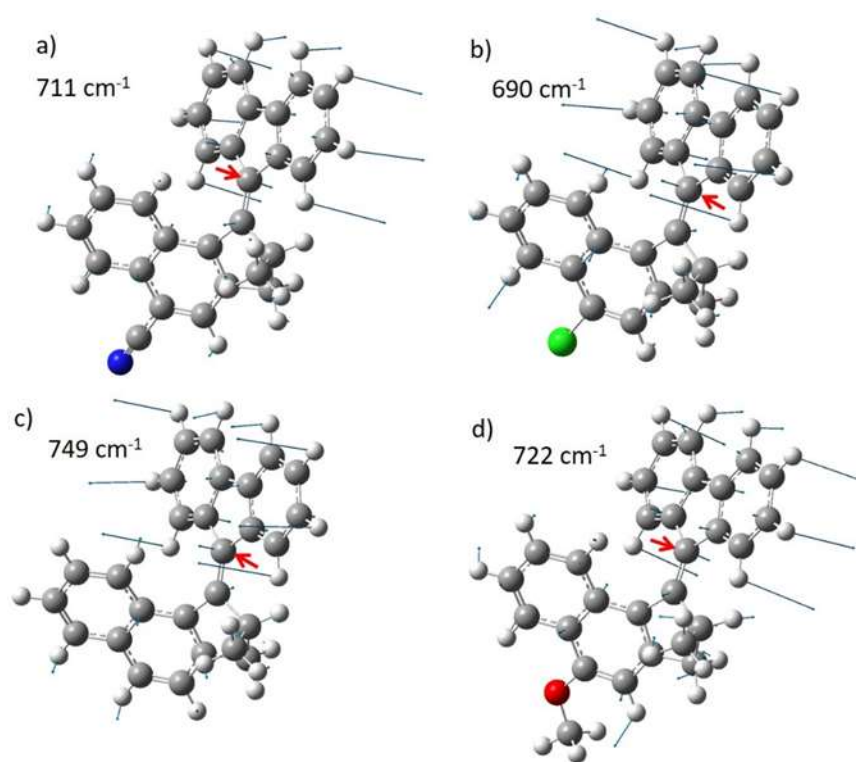


Figure S7. The pyramidalization mode (whose center is marked by red arrow) coupled to hydrogen-out-of-plane (HOOP) bending motion for the four motor derivatives a) $-\text{CN}$, b) $-\text{Cl}$, c) $-\text{H}$ and d) $-\text{OMe}$.

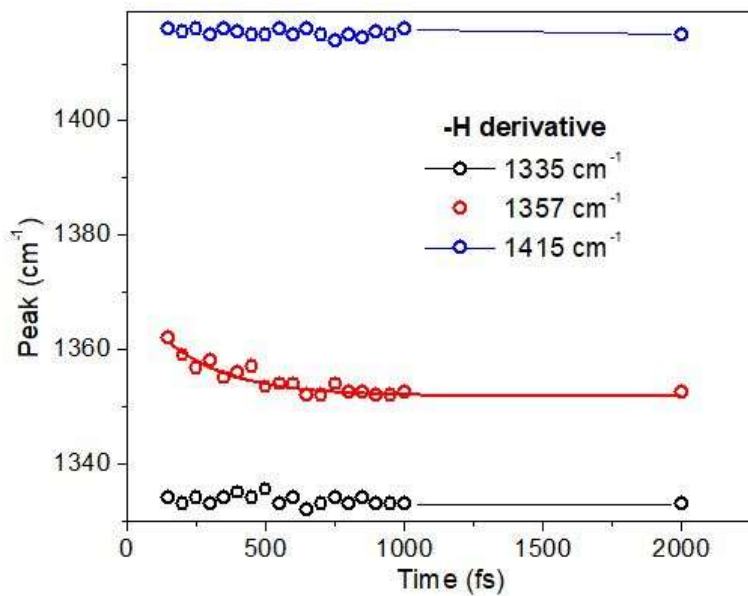


Figure S8 Time dependent FSRS Peak frequencies of -H derivative. Peak frequencies were obtained from sum of Gaussian fitting with fixed width and varying frequency.

Table S1. Relaxation times recovered from spectral shift dynamics in the dark state Transient absorption, FSRS frequency evolution; FSRS amplitude decay.

R	ESA Spectral shift dynamics	FSRS peak shift dynamics	FSRS peak area dynamics
OMe	---	---	---, 0.21 ps
H	1.2 ps	0.41 ps	0.28 ps, 1.2 ps
Cl	1.1 ps	0.53 ps	0.35 ps, 1.9 ps
CN	0.9 ps	0.35 ps	0.5 ps, 10.6 ps

References.

1. Pollard, M. M.; Meetsma, A.; Feringa, B. L., A Redesign of Light-Driven Rotary Molecular Motors. *Organic & biomolecular chemistry* **2008**, *6*, 507-512.
2. Conyard, J.; Cnossen, A.; Browne, W. R.; Feringa, B. L.; Meech, S. R., Chemically Optimizing Operational Efficiency of Molecular Rotary Motors. *Journal of the American Chemical Society* **2014**, *136*, 9692-9700.
3. Hall, C. R.; Conyard, J.; Heisler, I. A.; Jones, G.; Frost, J.; Browne, W. R.; Feringa, B. L.; Meech, S. R., Ultrafast Dynamics in Light-Driven Molecular Rotary Motors Probed by Femtosecond Stimulated Raman Spectroscopy. *Journal of the American Chemical Society* **2017**, *139*, 7408-7414.
4. Canrinus, T. R.; Lee, W. W.; Feringa, B. L.; Bell, S. E.; Browne, W. R., Supramolecular Low-Molecular-Weight Hydrogelator Stabilization of Sers-Active Aggregated Nanoparticles for Solution and Gas Sensing. *Langmuir* **2017**, *33*, 8805-8812.
5. Menges, F., Spectragryph-Optical Spectroscopy Software. *Version* **2017**, *1*, 2016-2017.
6. Frisch, M. J., et al. *Gaussian 16 Rev. C.01*, Wallingford, CT, 2016.
7. Merrick, J. P.; Moran, D.; Radom, L., An Evaluation of Harmonic Vibrational Frequency Scale Factors. *The Journal of Physical Chemistry A* **2007**, *111*, 11683-11700.